EARTHQUAKE ENGINEERING AND STRUCTURAL DYNAMICS, VOL. 21, 145–162 (1992)

DYNAMIC PILE–SOIL–PILE INTERACTION. PART II: LATERAL AND SEISMIC RESPONSE

NICOS MAKRIS AND GEORGE GAZETAS
Department of Civil Engineering, 212 Ketter Hall, State University of New York at Buffalo, NY 14260, U.S.A.

SUMMARY

A simplified three-step procedure is proposed for estimating the dynamic interaction between two vertical piles, subjected either to lateral pile-head loading or to vertically-propagating seismic S-waves. The starting point is the determination of the deflection profile of a solitary pile using any of the established methods available. Physically-motivated approximations are then introduced for the wave field radiating from an oscillating pile and for the effect of this field on an adjacent pile. The procedure is applied in this paper to a flexible pile embedded in a homogeneous stratum. To obtain analytical closed-form results for both pile-head and seismic-type loading pile–soil and soil–pile interaction are accounted for through a single dynamic Winkler model, with realistic frequency-dependent 'springs' and 'dashpots'. Final- and intermediate-step results of the procedure compare favourably with those obtained using rigorous formulations for several pile group configurations. It is shown that, for a *homogeneous* stratum, pile-to-pile interaction effects are far more significant under *head* loading than under *seismic* excitation.

INTRODUCTION

The dynamic stiffness of a group of vertical piles in any mode of vibration can not be computed by simply adding the stiffnesses of the individual piles, since each pile is affected not only by its own load, but also by the load and deflection of its neighbouring piles. Similarly, the seismic response of a pile group may differ substantially from the response of each individual pile taken alone, because of additional deformations transmitted from the adjacent piles. This pile-to-pile interaction is frequency-dependent, resulting from waves that are emitted from the periphery of each pile and propagate to 'strike' the neighbouring piles. Several researchers have developed a variety of numerical[1–7] and analytical[8,9] methods to compute the dynamic response of pile groups accounting for pile-to-pile interaction. A recent comprehensive review on the subject has been presented by Novak.[10]

In this paper the dynamic response of laterally-vibrating pile groups is investigated as a continuation of earlier work by the authors,[9] which dealt with axial vibration. Simplified closed-form analytical solutions are developed for the problem of *dynamic pile–soil–pile interaction* for two major types of loading:

(a) lateral harmonic force or moment at the pile cap ('inertial'-type loading);
(b) seismic excitation in the form of harmonic vertical incident shear waves ('kinematic' loading).

The obtained results are shown to be in agreement with rigorous solutions.

OUTLINE OF PROPOSED GENERAL METHOD

A general approximate method is proposed that involves the following *three* consecutive steps, schematically illustrated in Figure 1 (for 'inertial' type loading) and in Figure 2 (for 'kinematic' type loading):

Step 1. *The lateral deflection, $u_{11}(z)$, of a single (solitary) pile*, subjected to either lateral 'inertial' loads at its head or 'kinematic' seismic-wave deformations of the surrounding soil, is determined using the best procedure(s) available. For instance, one may use a dynamic finite-element code,[11–13] a boundary-element-type formulation,[2,7] a semi-analytical formulation[3,4,10,14] and a beam-on-Winkler-foundation method

0098–8847/92/020145–18$09.00

Received 28 May 1991
Revised 27 August 1991

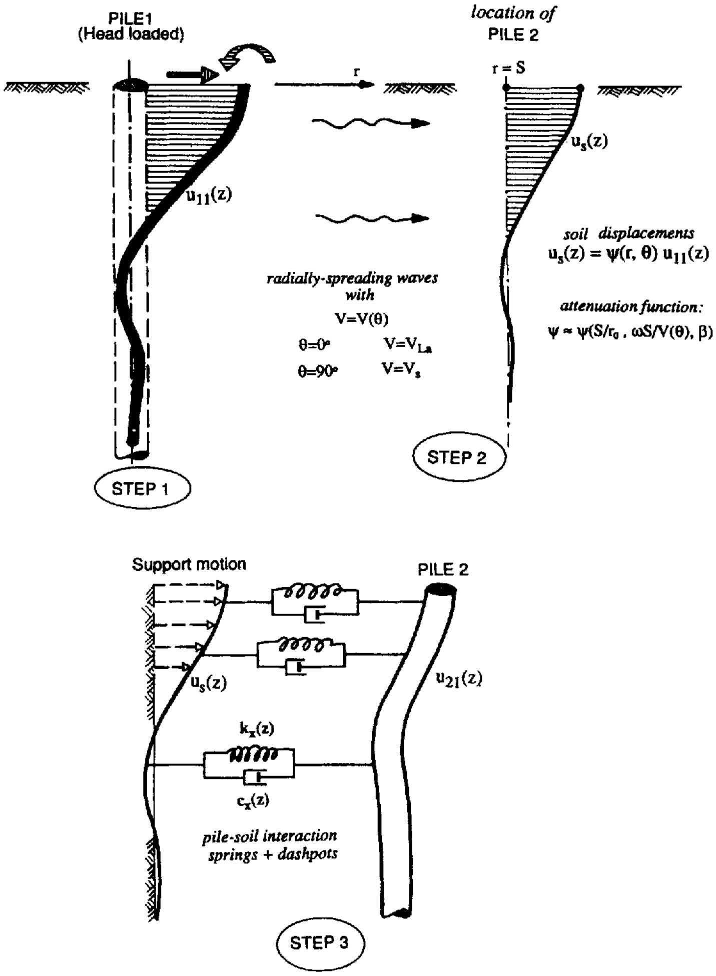

Figure 1. Schematic illustration of the developed 3-step procedure for computing the influence of PILE 1, deforming under harmonic lateral head loading, upon the adjacent PILE 2

along with pertinent complex-valued dynamic 'springs'[15] or dynamic 'p–y' curves.[16,17] Alternatively, even well-instrumented lateral pile load tests in the field, on a shaking table, or in the centrifuge could be conceivably used as a guide in constructing $u_{11}(z)$.[17–21] In this paper, we present results using a dynamic Winkler model to account for soil–pile interaction; this choice was not a necessity but stemmed *solely* from the need to derive *analytical* results for pile–soil–pile interaction in *closed form.* (Figure 2 illustrates the dynamic Winkler model utilized in Step 1 for computing the 'kinematic' response of a single pile.)

Step 2. This step begins by computing the *difference*, $\Delta u_{11} = u_{11} - u_{ff}$, between single pile deflections and free-field soil displacements. With 'inertial' loading this difference is just the deflection of the pile: $\Delta u_{11} = u_{11}$. For 'kinematic' loading, the response of the free-field soil, sketched in Figure 2, is computed by one-dimensional (1D) 'soil-amplification' methods. (Non-vertically-incident waves conceivably could be treated in the same way, by using 2D soil response methods, but this is not explored in this article.) This difference, $\Delta u_{11}(z)$ or simply $u_{11}(z)$, generates waves at all points along the pile. It is assumed that these waves spread out horizontally, as originally assumed in Novak's single pile method (e.g. Reference 15); their attenuation with distance r and 'angle of departure' θ is estimated using plane elastodynamic theory and assuming viscoelastic soil behaviour. Thus, at the *location* of pile 2, $r = S$, if this pile were not present, the arriving

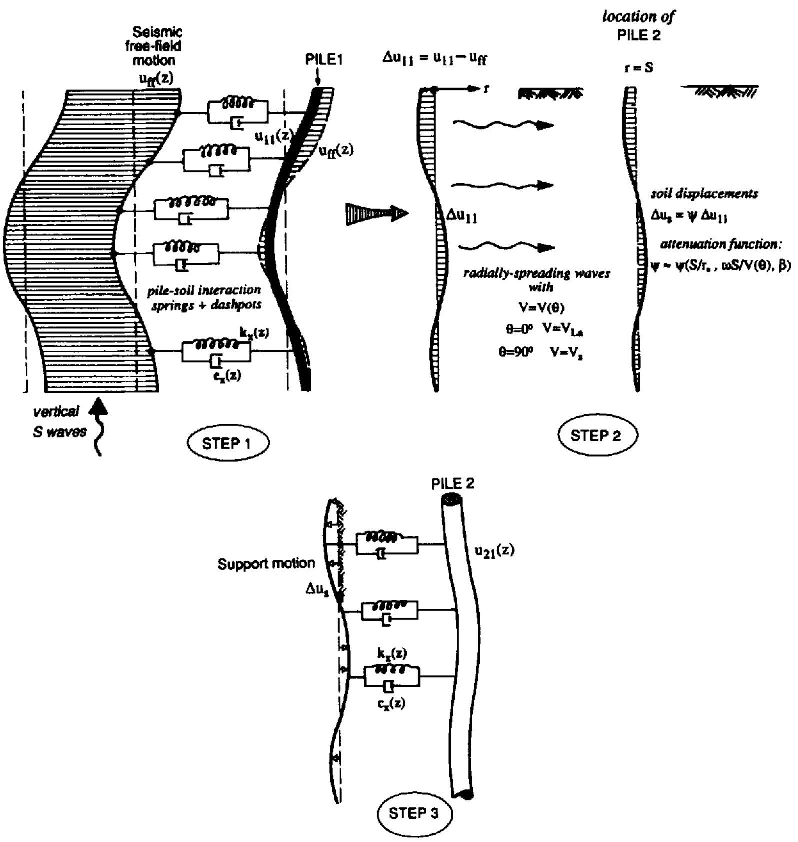

Figure 2. Schematic illustration of the developed 3-step procedure for computing the influence of PILE 1, deforming under seismic-type excitation, upon the adjacent PILE 2

attenuated waves would produce lateral soil displacements Δu_s (or simply u_s for head-loaded pile) determined as illustrated in Figures 1–2, and explained in the sequel.

Step 3. The presence of pile 2 will modify the arriving wave field $\Delta u_s(z)$ *or* $u_s(z)$, reflecting and diffracting the incoming waves. As a result, depending on its relative flexural rigidity and the vertical fluctuations of the arriving wave field, pile 2 may just follow closely the ground, experiencing displacements $u_{21}(z) \approx u_S(z)$ [long-flexible pile and smoothly-varying $u_s = u_S(z)$], or it may remain nearly still $u_{21}(z) \approx 0$ [rigid pile, rapidly fluctuating $u_S = u_S(z)$]. But in general its response $u_{21}(z)$ will be something in between these two extremes. To account in a simple practical way for this soil–pile interaction, we use a Beam-on-Dynamic-Winkler-Foundation (BDWF) model, in which the excitation takes the form of a support motion, equal to the attenuated displacement field $u_S(z)$ [*or* $\Delta u_s(z)$] of Step 2. As illustrated in Figures 1 and 2, the response of the pile-beam to this support motion is the desired response $u_{21}(z)$ of pile 2.

One of the main simplifications introduced herein is the decoupling of the 'mechanism' that transmits the motion in each of the three steps outlined above. Note that we do not directly connect the interacting piles by springs as was done by Nogami *et al.*[3] Once the source of the displacement in the soil is determined in Step 1, we use approximate wave equations to represent the motion in the free field. This is a very natural and effective way to represent the energy dissipation. Radiation damping, hysteretic soil damping and phase-difference effects play independently their role in the wave equation of the free field. Also note that Dobry and Gazetas[8] assumed that the pile-head deflection would be equal to the average of the soil induced displacement. This assumption may be quite good for vertical vibration, where the axial rigidity of the pile is usually significant, and the pile displacements are primarily the result of a rigid body motion. But for lateral vibration this assumption tends to exaggerate the pile-to-pile effect. By contrast the soil–pile interaction model used in Step 3 can be shown to provide a realistic solution to the problem. This general methodology is explained in detail below for a flexible pile under head loading and under seismic excitation.

HARMONIC EXCITATION AT THE PILE HEAD ('INERTIAL' RESPONSE)

Problem definition

Under lateral pile-head loading, only the upper portion of a flexible pile experiences significant deformation. The length of this portion, called 'active length', has been established for both static and dynamic loading.[12,13,22] Thus, there is hardly a need to distinguish between a floating and an end-bearing pile and the pile can be treated as an infinitely-long beam with no appreciable loss in accuracy. This beam is considered linear elastic with circular cross-section A_p, diameter d, second moment of area I_p, Young modulus E_p and mass density ρ_p.

The soil is modelled as a Winkler foundation resisting the lateral pile motion by *continuously-distributed frequency-dependent* linear springs k_x and dashpots c_x. The latter model the energy losses due to radiation of waves and due to hysteretic dissipation. Expressions for these coefficients are available in the literature[14,23] on the basis of which the following simple approximations are derived:

$$k_x \approx 1{\cdot}2E_s \tag{1}$$

$$c_x \approx 6a_0^{-1/4}\rho_s V_s d + 2\beta_s \frac{k_x}{\omega} \tag{2}$$

where E_s, V_s, β_s and ρ_s, are the Young's modulus, shear wave velocity, damping ratio and mass density of the soil; $m = \rho_p A_p$ is the mass per unit length of the pile; $a_0 = \omega d/V_s$.

Deflections of a single (solitary) pile—Step 1

With reference to Figure 1, dynamic equilibrium during harmonic steady-state motion $u_{11}(z) = U_{11}(z)\exp(\mathrm{i}\omega t)$ requires that

$$E_p I_p \frac{\mathrm{d}^4 U_{11}(z)}{\mathrm{d}z^4} + (k_x + \mathrm{i}\omega c_x - m\omega^2)U_{11}(z) = 0 \tag{3}$$

Applying Laplace transformation one gets

$$L\{U_{11}(z)\} = U'''_{11}(0)\frac{1}{s^4 + 4\lambda^4}1 + U''_{11}(0)\frac{s}{s^4 + 4\lambda^4} + U_{11}(0)\frac{s^3}{s^4 + 4\lambda^4} \tag{4}$$

where the prime denotes derivative with respect to z, and

$$\lambda = \left\{\frac{k_x + \mathrm{i}\omega c_x - m\omega^2}{4E_p I_p}\right\}^{1/4} \tag{5}$$

Laplace-inverting equation (4), while enforcing the boundary relations

$$\frac{U'''_{11}(o)}{16\lambda^3} + \frac{U''_{11}(o)}{8\lambda^2} = 0 \tag{6a}$$

$$-\frac{U'''_{11}(o)}{16\lambda^3} + \frac{U_{11}(o)}{4} = 0 \tag{6b}$$

which ensure finite displacement amplitude as z tends to infinity, one obtains the final solution:

$$u_{11}(z) = U_{11}(z)\mathrm{e}^{\mathrm{i}\omega t} = \frac{U_0}{2}\{(1 + i)\mathrm{e}^{-Rbz}\mathrm{e}^{\mathrm{i}(\omega t - Raz)} + (1 - i)\mathrm{e}^{-Raz}\mathrm{e}^{\mathrm{i}(\omega t + Rbz)}\} \tag{7}$$

where $U_0 = U_{11}(0)$ is the displacement amplitude at the pile head and

$$R = \left\{ \frac{(k_x - m\omega^2)^2 + (\omega c_x)^2}{(4E_p I_p)^2} \right\}^{1/8} \tag{8}$$

$$a = \cos\frac{\theta}{4} + \sin\frac{\theta}{4}, \quad b = \cos\frac{\theta}{4} - \sin\frac{\theta}{4} \tag{9}$$

$$\theta = \arctan\left(\frac{\omega c_x}{k_x - m\omega^2} \right) \quad 0 < \theta < \frac{\pi}{2} \tag{10}$$

Observe that if damping were neglected ($c_x = 0$) equation (7) would reduce to a standing wave

$$u_{11}(z) = U_0 e^{-\lambda z}(\sin \lambda z + \cos \lambda z) e^{i\omega t} \tag{11}$$

and λ reduces from a complex to a real number

$$\lambda = \left\{ \frac{k_x - m\omega^2}{4E_p I_p} \right\}^{1/4} \tag{12}$$

Equation (11) is of the same form as the static solution,[24] but here of course $\lambda = \lambda(\omega)$. This special case has been discussed by Wolf.[25]

As an example, Figure 3 compares the distribution with depth of the (normalized) amplitude given by equations (7) and (11), as well as the phase-angle differences between a point on the pile at depth z and the pile head. Notice that for the chosen E_p/E_s ratio, 1000 and $a_0 = 0{\cdot}3$ the pile 'active' length extends to about 9 diameters from the surface. Moreover, equation (7) predicts that the motion would become substantially out of phase only at a depth where the amplitude is at most 5 to 10 per cent of the head amplitude. Consequently, although the damped and undamped models give a completely different result for the nature of the waves propagating down the pile, the induced displacement distributions to the soil are similar. In the sequel this observation simplifies considerably the algebra in analysing the pile-to-pile interaction, where we make use of equation (11) rather than of equation (7).

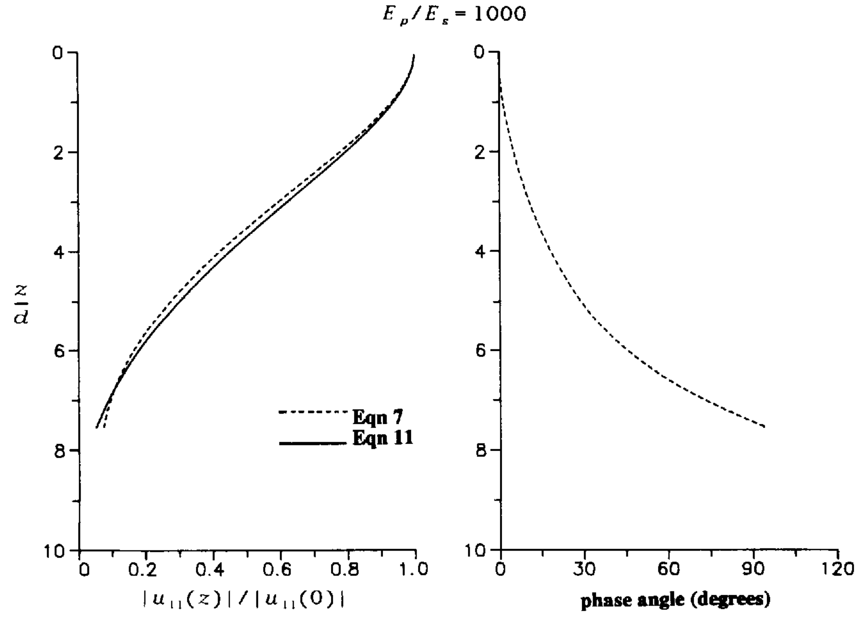

Figure 3. Normalized deflection amplitude and phase angle of a fixed-head pile under lateral loading, at a dimensionless frequency $a_0 = 0{\cdot}3$. The continuous line is the result of equation (11) (no damping) whereas the dashed line is the result of equation (7)

Next, using the foregoing pile deflection as a displacement 'source' we determine the soil displacements, u_s, at a distance $r = S$.

Attenuation of soil displacement away from 'source' pile—Step 2

P- and S-waves are emitted from the oscillating pile, travelling in all directions and being reflected from the free surface of the soil. A rigorous formulation of this 3D problem would be a formidable task, especially if one foresees an extension to layered soils. Several approximate models, based on 1D, 2D or 3D wave propagation idealizations, are nevertheless available.[14,15,26,27] They are reviewed briefly below.

Berger *et al.*[26] assumed that a horizontally moving pile cross-section would generate solely 1D P-waves travelling in the direction of shaking and 1D SH-waves travelling in the direction perpendicular to shaking. Although the simplicity of this model is attractive, the constraints imposed from the 1D consideration lead to frequency-independent radiation damping which achieves unrealistically high values when the Poisson's ratio ν approaches 0·5. Novak *et al.*[15] developed a 2D model by solving the problem of a soil slice of infinite extent subjected to horizontal oscillations from a rigid circular inclusion [Figure 4(a)]. The restriction of vertical deformations ($\varepsilon_z = 0$) corresponds to a plane-strain problem and a 2D solution. Roesset and co-workers[23,27] verified the validity of this 2D model. They used a 3D FE formulation for the developing soil reactions against pile displacements. An alternative approximate 2D plane-strain model, presented by Gazetas and Dobry[14] assumes that compression–extension waves propagate in the two quarter-planes along the direction of loading while shear waves are generated in the two quarter-planes perpendicular to the direction of loading [Figure 4(b)]. The apparent phase velocity of the compression–extension waves is approximated by the so-called 'Lysmer's analogue' wave velocity[14] $V_{La} = [3{\cdot}4/\pi(1-\nu)]\,V_s$. The shear waves propagate, of course, with velocity V_s.

The models of Gazetas and Dobry[14] and of Novak *et al.*[15] are both utilized herein. According to the first, at a distance r from the oscillating pile and an angle θ from the direction of loading the displacement field can be simply expressed as

$$u_s(r, \theta, z) = U_S \exp(i\omega t) = \psi(r, \theta) u_{11}(z) \tag{13}$$

where u_{11} is given by equation (11) and $\psi(r, \theta)$ is the attenuation function (still to be determined). It is sufficient to compute $\psi(r, \theta)$ only for $\theta = 0$ and $\theta = \pi/2$ and then use the approximation

$$\psi(r, \theta) \approx \psi(r, 0)\cos^2\theta + \psi\left(r, \frac{\pi}{2}\right)\sin^2\theta \tag{14}$$

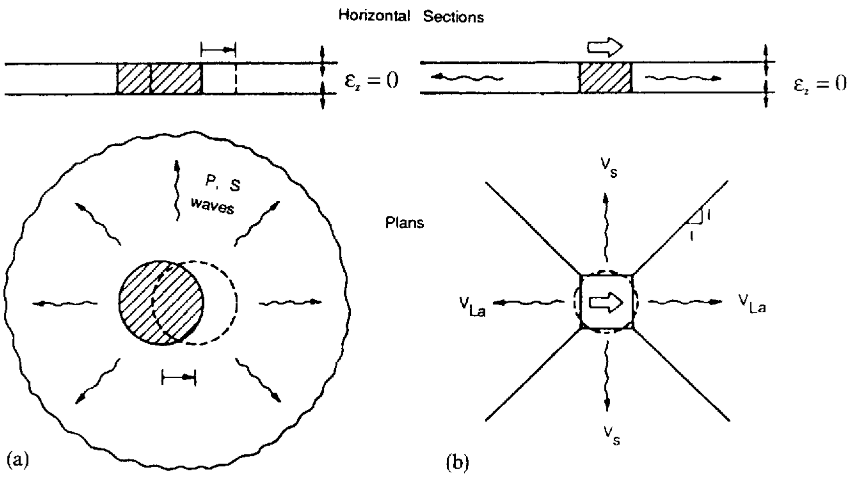

Figure 4. Schematic representation of 2D radiation model: (a) 'rigorous' plane-strain model of Novak *et al.*[15]; (b) simplified plane-strain model of Gazetas and Dobry[14]

to obtain a very good estimate for any arbitrary angle θ.[2,7,28] The following approximate expressions for $\psi(r, 0)$ and $\psi(r, \pi/2)$ have been developed in Reference [8]:

$$\psi(r,0) = \frac{\sqrt{r_0}}{\sqrt{r}} \exp\left(\frac{-\beta\omega(r - r_0)}{V_{La}}\right) \exp\left(\frac{-i\omega(r - r_0)}{V_{La}}\right) \tag{15a}$$

$$\psi\left(r, \frac{\pi}{2}\right) = \frac{\sqrt{r_0}}{\sqrt{r}} \exp\left(\frac{-\beta\omega(r - r_0)}{V_s}\right) \exp\left(\frac{-i\omega(r - r_0)}{V_s}\right) \tag{15b}$$

The factor $1/\sqrt{r}$ represents the reduction in amplitude due to geometric spreading (radiation) of waves while the factors $\exp(-\beta\omega r/V)$ express the amplitude reduction due to hysteresis in the soil. The third factors describe a radially-propagating wave with phase velocity V_{La} for $\theta = 0$, and V_s for $\theta = \pi/2$.

Although the attenuation expressions from equations (14)–(15) appear to be extremely simple, the results obtained are very close to the more sophisticated solution that we derived:

$$\begin{aligned}\psi(r,\theta) = {} & \left\{\psi_1\left[H_0^{(2)}(\gamma r) \frac{1}{\gamma r} H_1^{(2)}(\gamma r)\right] + \psi_2\left[\frac{1}{\gamma r} H_1^{(2)}(\delta r)\right]\right\} \cos^2\theta \\ & + \left\{\psi_1\left[\frac{1}{\gamma r} H_1^{(2)}(\gamma r)\right] + \psi_2\left[\frac{\delta}{\gamma} H_0^{(2)}(\delta r) - \frac{1}{\gamma} r H_1^{(2)}(\delta r)\right]\right\} \sin^2\theta\end{aligned} \tag{16}$$

where

$$\gamma = \frac{\omega}{V_p}, \qquad \delta = \frac{\omega}{V_s} \tag{17a}$$

and

$$\psi_1 = \frac{2H_1^{(2)}(\delta r_0) - \delta r_0 H_0^{(2)}(\delta r_0)}{H_0^{(2)}(\gamma r_0) H_1^{(2)}(\delta r_0) - \delta r_0 H_0^{(2)}(\gamma r_0) H_0^{(2)}(\delta r_0) - \dfrac{\delta}{\gamma} H_0^{(2)}(\delta r_0) H_1^{(2)}(\gamma r_0)} \tag{17b}$$

$$\psi_2 = \frac{2H_1^{(2)}(\gamma r_0) - \gamma r_0 H_0^{(2)}(\gamma r_0)}{H_0^{(2)}(\gamma r_0) H_1^{(2)}(\delta r_0) - \delta r_0 H_0^{(2)}(\gamma r_0) H_0^{(2)}(\delta r_0) - \dfrac{\delta}{\gamma} H_0^{(2)}(\delta r_0) H_1^{(2)}(\gamma r_0)} \tag{17c}$$

in which $H_0^{(2)}$ denotes the zero-order second-kind Hankel function and V_p is the soil P-wave velocity. Figure 5 compares the real and imaginary part of equations (14) and (16), plotted as functions of the horizontal distance r normalized by the pile diameter d. The differences are rather small and use of either one set in the subsequent analysis *does* indeed lead to quite similar results.

We use equation (13) in conjunction with equation (14) to describe the soil displacement field.

Interaction of 'receiver' pile with arriving waves—Step 3

Consider now a second ('receiver') pile, 2, located at a distance $r = S$ from the 'source' pile 1. The soil displacement field computed in Step 2 [equation (13)] affects pile 2. The flexural rigidity of the pile, however, tends to resist this deflection, and the result is a modified motion at its soil–pile interface. This physical phenomenon is in a sense the reverse of that of Step 1. In Step 1 the 'source' pile induces displacements on the soil, whereas in Step 3 the soil induces displacements on the 'receiver' pile.

To describe the mechanics of this loading we utilize once again the generalized Winkler model of Step 1. But now it is *the supports of the 'springs' and 'dashpots'* that *undergo the induced soil displacement* $u_s(r, \theta, z)$ and exert along the pile a distributed load equal to the net displacement $(u_s - u_{21})$ times the impedance $k_x + i\omega C_x$, where $u_{21} = u_{21} \exp(i\omega t)$ denotes the deflexion of the 'receiver' pile 2. Dynamic equilibrium for

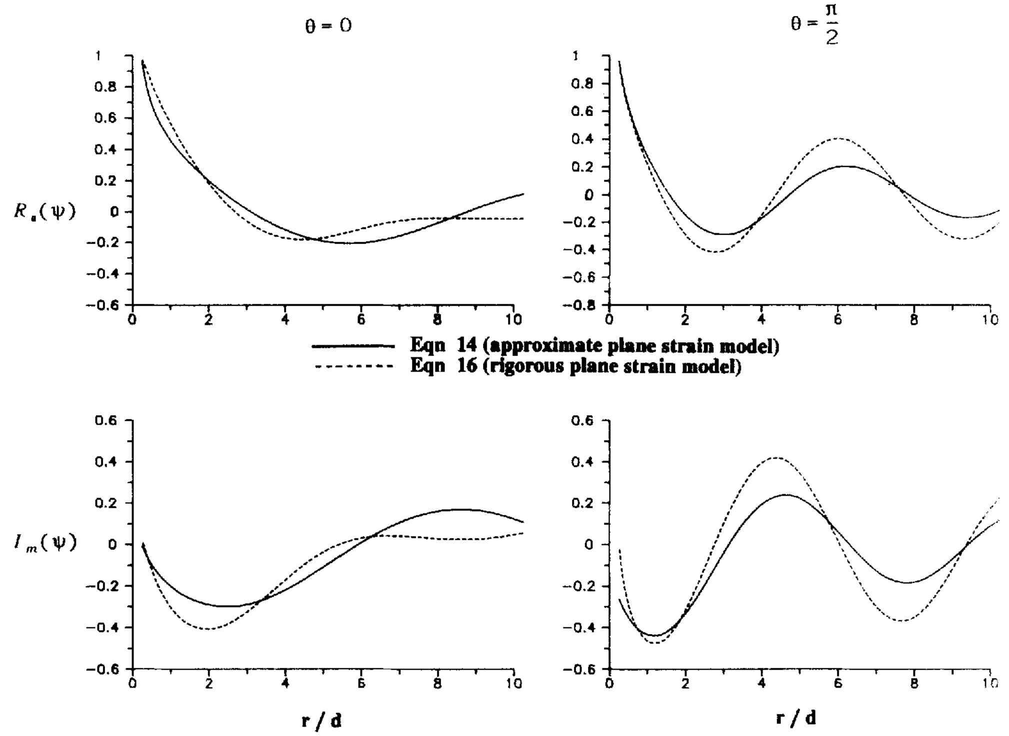

Figure 5. Real and imaginary part of attenuation factor as a function of distance: comparison between the approximate model by Gazetas and Dobry[14] (equation (14)—continuous line) and the plane-strain model by Novak *et al.*[15] (equation (16)—dashed line)

pile 2 gives

$$E_p I_p \frac{d^4 U_{21}}{dz^4} + (k_x + i\omega c_x - m\omega^2) U_{21} = (k_x + i\omega c_x) U_s \tag{18}$$

or, after substituting U_S from equation (13) into equation (18),

$$E_p I_p \frac{d^4 U_{21}}{dz^4} + (k_x + i\omega c_x - m\omega^2) U_{21} = (k_x + i\omega c_x) \psi(r, \theta) U_0 e^{-\lambda z} (\cos \lambda z + \sin \lambda z) \tag{19}$$

The solution of equation (19) is also obtained using the Laplace transform technique. After lengthy calculations one obtains

$$U_{21}(z) = \frac{3}{4} \psi(r, \theta) \left(\frac{k_x + i\omega c_x}{k_x + i\omega c_x - m\omega^2} \right) U_0 e^{-\lambda z} \left(\cos \lambda z + \sin \lambda z + \frac{2}{3} \lambda z \sin \lambda z\right) \tag{20}$$

which is the sought response of the 'receiver' pile. It is useful to express the pile-to-pile interaction through the *dynamic interaction factor*[2,7,8,9]

$$\alpha_{21} = \frac{\text{additional head deflection of pile 2 caused by pile 1}}{\text{head deflection of pile 1}} \tag{21a}$$

From equations (20) and (11) one obtains for $z = 0$

$$\alpha_{21} = \frac{3}{4} \psi(r, \theta) \frac{k_x + i\omega c_x}{k_x + i\omega c_x - m\omega^2} \tag{21b}$$

Equation (21b) is sufficient for computing the lateral response of any group of piles, once the single pile impedance is available. The computation of the group 'efficiency' using interaction factors has been extensively presented elsewhere.[2,7,8,28,29]

One of the published solutions derived with rigorous formulations is by Kaynia and Kausel,[2] who use closed-form Green's functions as the basis of computing the dynamic impedance of the group. Using Kaynia and Kausel's single pile impedance the group impedances are calculated utilizing the interaction factors of equation (21b) [in conjunction with equations (14)–(15)]. Figures 6 and 7 compare the stiffness and damping computed with the two methods for a 2 by 2 and a 3 by 3 pile group, for two separation distances ($s/d = 5$ and 10). The results are presented in a normalized form where the group dynamic stiffness and damping are divided by the sum of the static stiffnesses of the individual (identical) piles in the group, and are plotted versus the dimensionless frequency a_0. The two methods are in satisfactory agreement. Note that graphs similar to those of Figures 6 and 7 were presented by Dobry and Gazetas (Figures 11 and 12 of Reference 8), where they compared their results with the same rigorous solution of Kaynia and Kausel. In Reference 8 Step 3 was not taken into consideration and the interaction factor was merely: $\alpha_{21} = \psi(r, \theta)$. For the 2×2 pile group (Figure 6 of present paper and Figure 11 of Reference 8), no significant difference between the two approximate methods is observed. However, for the 3×3 pile group (Figure 7 of present paper and Figure 12

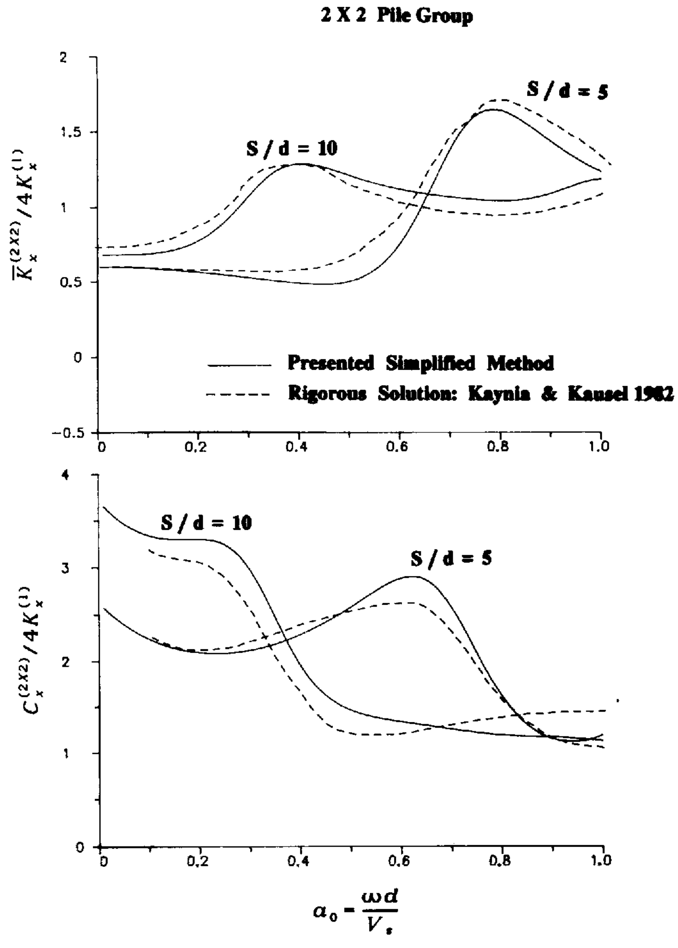

Figure 6. Dynamic stiffness and damping group factors as function of frequency: comparison of presented method with rigorous solution of Kaynia and Kausel for a 2×2 square group of rigid-capped piles in a homogeneous halfspace ($E_p/E_s = 1000$, $\rho_p/\rho_s = 1{\cdot}42$, $L/d = 15$, $\nu = 0{\cdot}4$, $\beta = 0{\cdot}05$)

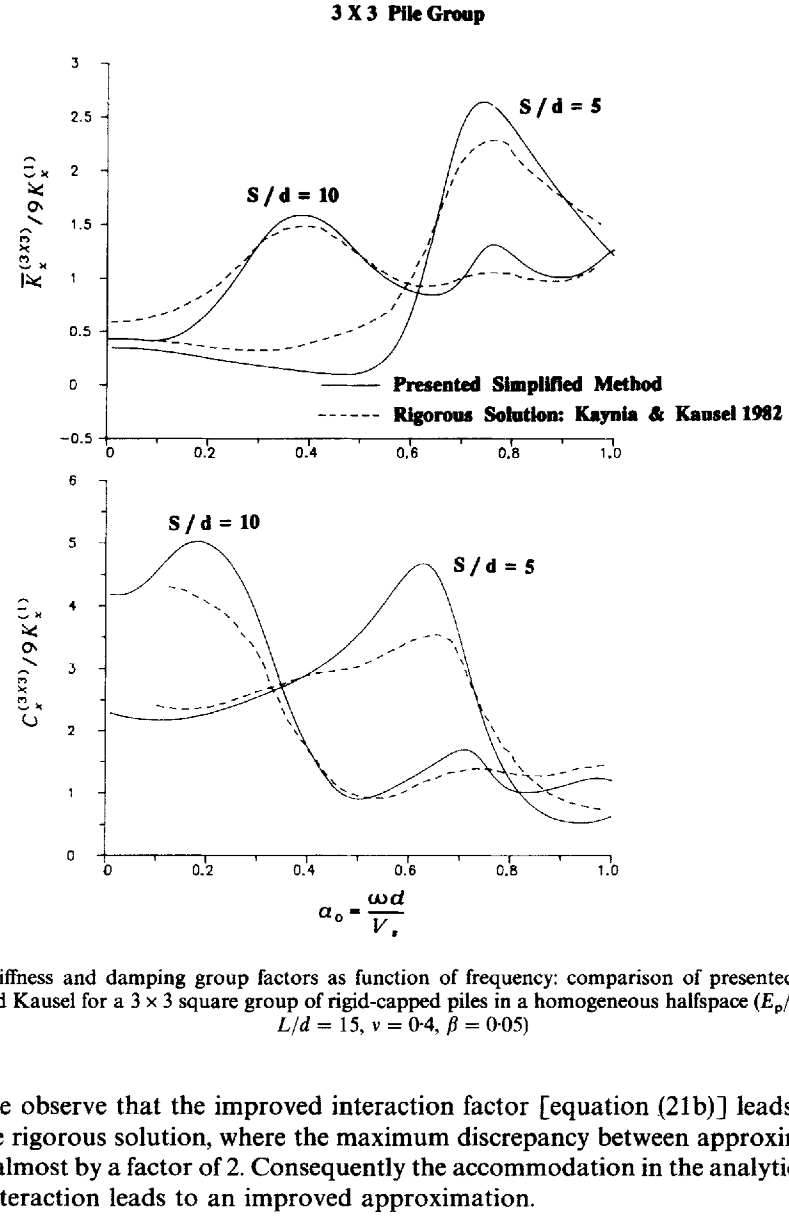

Figure 7. Dynamic stiffness and damping group factors as function of frequency: comparison of presented method with rigorous solution of Kaynia and Kausel for a 3 × 3 square group of rigid-capped piles in a homogeneous halfspace ($E_p/E_s = 1000$, $\rho_p/\rho_s = 1{\cdot}42$, $L/d = 15$, $\nu = 0{\cdot}4$, $\beta = 0{\cdot}05$)

of Reference 8), we observe that the improved interaction factor [equation (21b)] leads to results that are much closer to the rigorous solution, where the maximum discrepancy between approximate and rigourous results is reduced almost by a factor of 2. Consequently the accommodation in the analytical procedure of the *Step*-3 soil–pile interaction leads to an improved approximation.

HARMONIC EXCITATION BY VERTICAL S-WAVES (KINEMATIC RESPONSE)

Problem definition

The response of piles and pile groups to vertically propagating S-waves has also been the subject of research,[2, 30–34] although not as extensively as the head-loading problem. With such an excitation a pile would undergo deflections over its entire length; hence the *infinite* beam model must be replaced with a *finite* one. For an end-bearing pile the analysis simplifies considerably because the displacement of the pile tip is equal to the imposed base displacement. However, with floating piles the displacement of the tip is not known *a priori* and it depends on the wavelength of the input motion.

The study presented herein concentrates only on the response of end-bearing pile groups, excited by a vertically incident S-wave. Pile characteristics remain the same, as does the spring–dashpot system that reproduces the pile–soil interplay. In the following calculations 'fixed-head' conditions (i.e. zero top rotation) are assumed for the pile, but of course the method can treat as easily other boundary conditions. The pile tip is assumed pinned at the base, following the base motion without separation.

Displacement of single (solitary) pile—Step 1

For flexible piles and low frequencies of incoming waves (large wavelengths) the pile follows closely the oscillating free field. In general, however, because of its bending rigidity, the pile tends to resist the induced deflections. Schematically, the free-field and pile deformation are presented in Figure 2. Let $u_g = U_g \exp(i\omega t)$ describe the base motion, $u_{11} = U_{11}\exp(i\omega t)$ the pile deflection and $u_{ff} = U_{ff}\exp(i\omega t)$ the free-field horizontal displacement. Dynamic equilibrium under steady-state conditions gives

$$E_p I_p \frac{d^4 U_{11}}{dz^4} + m\omega^2 U_{11} - (k_x + i\omega c_x)(U_{ff} - U_{11}) = 0 \tag{22}$$

in which U_{ff} is determined from the theory of one-dimensional wave propagation (e.g. Roesset[35]) with boundary conditons: zero shear stresses at the free surface and displacement at the base equal to the induced base displacement U_g.

For the linear hysteretic soil assumed herein, the total free-field displacement is

$$u_{ff}(z) = \left(\frac{U_g}{\cos \dfrac{\omega}{V_s^*} L} \right) \cos\left(\frac{\omega}{V_s^*} z \right) e^{i\omega t} \tag{23}$$

where U_g is the amplitude of the harmonic base displacement and $V_s^* = V_s\sqrt{1 + 2i\beta}$. Substituting equation (23) into equation (22) leads to

$$E_p I_p \frac{d^4 U_{11}}{dz^4} + (k_x + i\omega c_x - m\omega^2) U_{11} = (k_x + i\omega c_x) U_g \frac{\cos \delta z}{\cos \delta L} \tag{24}$$

in which the 'wave number' δ is given by equation (17a) and V_s is replaced by V_s^*.

The total solution of this equation, given in equation (25), is the sum of the homogeneous and a particular solution. (The homogeneous equation is identical to equation (3) but it now applies to a beam of finite length L.)

$$U_{11}(z) = e^{\lambda z}(A\cos\lambda z + B\sin\lambda z) + e^{-\lambda z}(C\cos\lambda z + D\sin\lambda z) + U_g \Gamma \frac{\cos\delta z}{\cos\delta L} \tag{25}$$

where λ is given by equation (5) and

$$\Gamma = \frac{k_x + i\omega c_x}{E_p I_p \delta^4 + k_x + i\omega c_x - m\omega^2} \tag{26}$$

The constants A, B, C, D are determined from the pile boundary conditions. At the soil surface: the slope of the pile is zero and the shear force is equal to the inertia force of the above-ground mass. At the pile tip: moment and relative displacement are zero. The constants A, B, C, D are then derived by solving the system

$$\begin{bmatrix} 1 & 1 & -1 & 1 \\ 1 - \dfrac{M\omega^2}{2\lambda^3 EI} & -1 & -\left[1 + \dfrac{M\omega^2}{2\lambda^3 EI}\right] & -1 \\ -2e^{\lambda L}\sin\lambda L & 2e^{\lambda L}\cos\lambda L & 2e^{-\lambda L}\sin\lambda L & -2e^{-\lambda L}\cos\lambda L \\ e^{\lambda L}\cos\lambda L & e^{\lambda L}\sin\lambda L & e^{-\lambda L}\cos\lambda L & e^{-\lambda L}\sin\lambda L \end{bmatrix} \begin{Bmatrix} A \\ B \\ C \\ D \end{Bmatrix} = \begin{Bmatrix} 0 \\ \dfrac{M\omega^2}{2\lambda^3 EI} U_g\left[\dfrac{\Gamma}{\cos\delta L} - 1\right] \\ U_g\left(\dfrac{\delta^2}{\lambda^2}\right)\Gamma \\ U_g(1 - \Gamma) \end{Bmatrix} \tag{27}$$

where M is the mass of the superstructure corresponding to one pile. For the kinematic solution M is set equal to zero. Note that the arguments of the *sine* and *cosine* functions in the above matrices are *complex* numbers owing to the presence of damping.

Parenthetically, it is noted that solution to an equation similar to equation (24), but with real rather than complex coefficients, was presented by Flores-Berrones and Whitman,[32] who dropped the homogeneous solution using the argument that the motion is steady-state. This is not exact, since equation (24) (or equation (21) of Reference 32) is a differential equation with respect to depth z and not to time t. Consequently, the homogeneous part of the solution is present even if the motion is harmonic, steady-state. Nevertheless, for most practical cases of interest, the participation of the homogeneous solution is not as important to the total solution and can indeed be neglected. This result is illustrated in Figure 8, where the displacement amplitude and phase angle difference of the displacements corresponding to the particular, the homogeneous and the total solution are plotted versus depth. Accordingly, in the sequel, the participation of the homogeneous solution is ignored and the pile deflection is approximated by

$$U_{11}(z) \approx U_{\mathrm{g}}\left(\Gamma \frac{\cos \delta z}{\cos \delta L}\right) = \Gamma U_{\mathrm{ff}}(z) \tag{28}$$

The ratio of pile to soil total displacement is thus

$$\Gamma = \frac{U_{11}}{U_{\mathrm{ff}}} \tag{29}$$

Figure 9 plots the absolute value of Γ versus frequency and compares the result obtained from the presented method with a rigorous solution used by Ke Fan *et al.*[34] for $E_{\mathrm{p}}/E_{\mathrm{s}} = 1000$ and 10 000. The agreement is very good indeed.

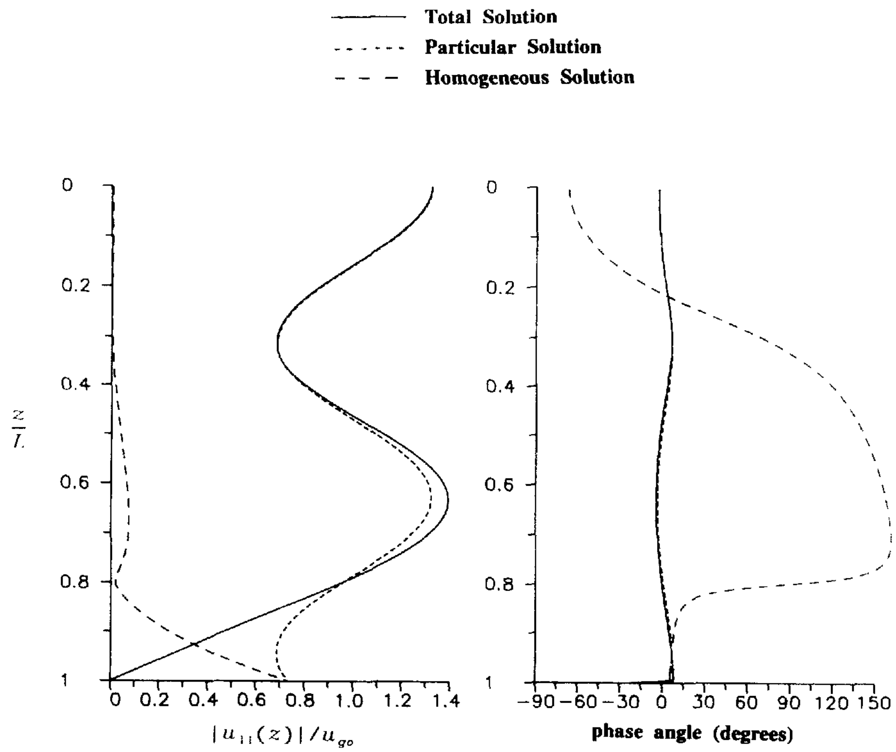

Figure 8. Pile deflection due to harmonic vertical S-waves at dimensionless frequency $a_0 = 0{\cdot}3$: amplitude and phase angle corresponding to the homogeneous, the particular and the total solution to the governing equation (24)

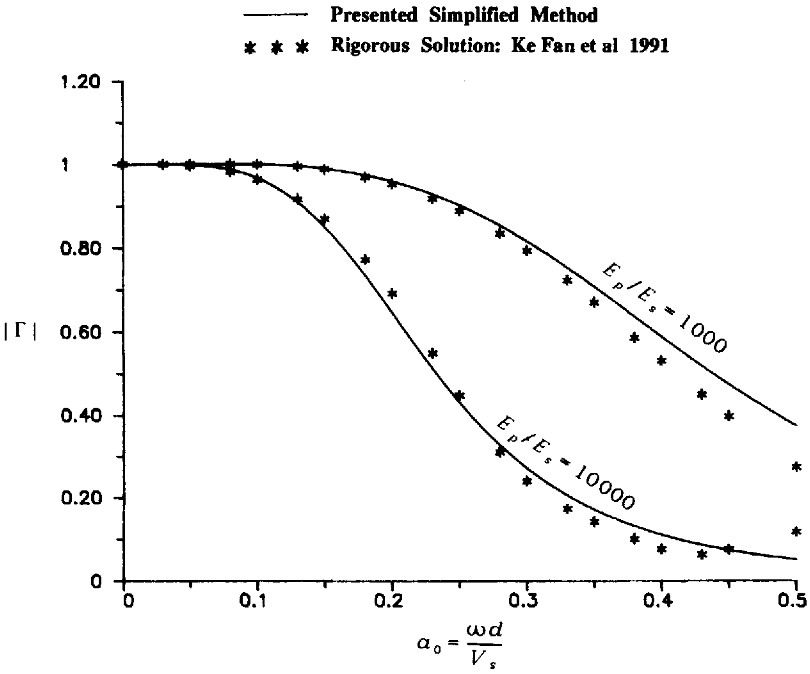

Figure 9. Normalized kinematic seismic response of single fixed-head pile: comparison of presented method with rigorous results by Ke Fan *et al.* ($\rho_p/\rho_s = 1{\cdot}42$, $L/d = 20$, $\nu = 0{\cdot}4$, $\beta = 0{\cdot}05$)

Diffracted soil displacement-field—Step 2

Equation (29) shows that the disparity between pile and soil deflection is controlled by the factor Γ. As the frequency approaches zero, Γ tends to 1 and therefore there is no difference between pile and soil displacement. As the frequency increases, Γ changes in both magnitude and phase. Therefore, a difference is created between pile response and free-field motion. *The pile-to-pile interaction is the result of the existence of this difference* $\Delta u_{11} = u_{11} - u_{ff}$ in Figure 2. Indeed, this difference perturbs the seismic wave field: new waves emanate from the pile–soil interface and spread outward, attenuating in the process. This diffracted wave field is described with the displacement at distance r and angle θ:

$$\Delta u_s = \psi(r, \theta)\Delta u_{11} = \psi(r, \theta)u_g(\Gamma - 1)\frac{\cos \delta z}{\cos \delta L} \tag{30}$$

where $\psi(r, \theta)$ is given again by equation (14).

Interaction of 'receiver' pile with waves diffracted by 'source' pile—Step 3

To determine the additional displacement that a neighbouring pile *2* located at distance $r = S$ experiences when it is struck by this diffracted wave field, we proceed exactly as in Step 3 of the head-loading case. Soil–pile interaction is modelled by springs and dashpots, the supports of which undergo displacement Δu_s. Thus, in the dynamic equilibrium equation, the displacement in the right-hand (forcing) term of equation (18) is now replaced by equation (30)

$$E_p I_p \frac{d^2 U_{21}}{dz^4} + (k_x + i\omega c_x - m\omega^2)U_{21} = k_x + i\omega c_x)\psi(r, \theta)U_g(\Gamma - 1)\frac{\cos \delta z}{\cos \delta L} \tag{31}$$

The solution

$$U_{21}(z) = \psi(r, \theta)\left\{e^{\lambda z}(A_1 \cos \lambda z + B_1 \sin \lambda z) + e^{-\lambda z}(C_1 \cos \lambda z + D_1 \sin \lambda z) + U_g\Gamma(\Gamma - 1)\frac{\cos \delta z}{\cos \delta L}\right\} \tag{32}$$

where λ is given again by equation (5) and A_1, B_1, C_1 and D_1 are new integration constants to be determined from the boundary conditions of pile 2. Again, however, the participation of the homogeneous solution is found to be negligible and only the particular solution is kept. Consequently, the additional displacement of pile 2 arising from the diffracted waves is approximated as

$$U_{21}(z) \approx \psi(r, \theta) U_g \Gamma(\Gamma - 1) \frac{\cos \delta z}{\cos \delta L} \tag{33}$$

Equation (21) yields the following expression for the interaction factor $\bar{\alpha}_{21} = U_{21}(z)/U_{11}(z)$ in *seismic* loading:

$$\bar{\alpha}_{21} \approx \psi(r, \theta)(\Gamma - 1) \tag{34}$$

Poulos' superposition procedure[29], verified for dynamic loading by Kaynia and Kausel[2] and Sanchez-Salinero,[28] can then be applied readily to determine the group response.

The following example computes the group displacement of 1 by 3 pile groups.

ILLUSTRATIVE EXAMPLE AND COMPARISON

We consider three identical piles in a row connected by a rigid cap restricted against rotation and subjected to seismic excitation. Let $U_1 = U_2 = U_3$ be the total displacement of the three piles equal to the group displacement, $U_G = U^{(1\times 3)}$, and F_1, F_2 and F_3, the forces that develop at their heads. Since the pile cap is considered massless, equilibrium of the cap requires that

$$F_1 + F_2 + F_3 = 0 \tag{35}$$

By superposition, the total displacement of each pile is the sum of:

(a) the seismic displacement of the single (solitary) pile;
(b) the additional displacements arising from the motions transmitted by the other two piles due to kinematic deformation;
(c) the displacement due to its own head loading, from force F_1 *or* F_2 *or* F_3;
(d) the additional displacements transmitted from the other two piles deforming under their head loading. (Apparently (a) and (b) are 'kinematic' effects, while (c) and (d) are inertia effects.)

Accordingly, for pile 1 we get

$$U_1 = U^{(1\times 3)} = U_{11} + \bar{\alpha}_{12} U_{22} + \bar{\alpha}_{13} U_{33} + \frac{F_1}{k_x^{(1)}} + \alpha_{12} \frac{F_2}{k_x^{(1)}} + \alpha_{13} \frac{F_3}{k_x^{(1)}} \tag{36}$$

where $U_{11} = U_{22} = U_{33}$ is the seismic displacement of the single (solitary) pile [equation (28)], $\bar{\alpha}_{12}$ and $\bar{\alpha}_{13}$ are the interaction factors for seismic loading [equation (34)], α_{12} and α_{13} are the interaction factors for inertial loading [equation (21)] and $k_x^{(1)}$ is the dynamic stiffness of the single pile. For piles 2 and 3 we get two more equations identical to equation (36) where indices 1, 2 and 3 permute. These equations together with equation (35) form a system of four equations with four unknowns $U^{(1\times 3)}$, F_1, F_2 and F_3.

$$\begin{bmatrix} 1 & -1 & -\alpha_{12} & -\alpha_{13} \\ 1 & -\alpha_{21} & -1 & -\alpha_{23} \\ 1 & -\alpha_{31} & -\alpha_{32} & -1 \\ 0 & 1 & 1 & 1 \end{bmatrix} \begin{Bmatrix} \dfrac{U^{(1\times 3)}}{U_{11}} \\ \dfrac{F_1}{k_x^{(1)} U_{11}} \\ \dfrac{F_2}{k_x^{(1)} U_{22}} \\ \dfrac{F_3}{k_x^{(1)} U_{33}} \end{Bmatrix} = \begin{Bmatrix} 1 + \bar{\alpha}_{12} + \bar{\alpha}_{13} \\ 1 + \bar{\alpha}_{21} + \bar{\alpha}_{23} \\ 1 + \bar{\alpha}_{31} + \bar{\alpha}_{32} \\ 0 \end{Bmatrix} \tag{37}$$

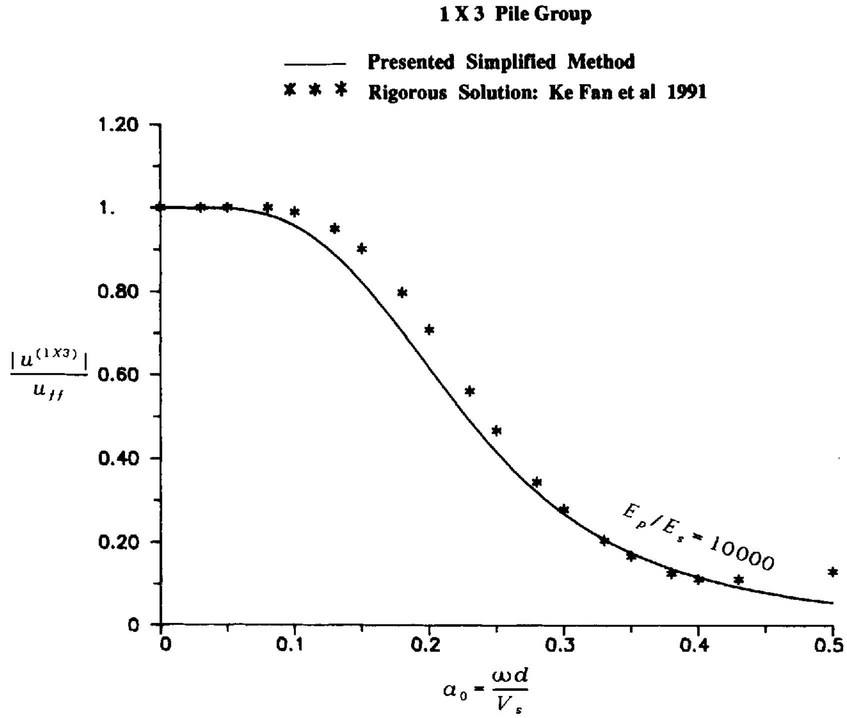

Figure 10. Normalized kinematic seismic response of 1 × 3 fixed-head pile group: comparison of presented method with rigorous results by Ke Fan *et al.* ($\rho_p/\rho_s = 1{\cdot}42$, $L/d = 20$, $\nu = 0{\cdot}4$, $\beta = 0{\cdot}05$)

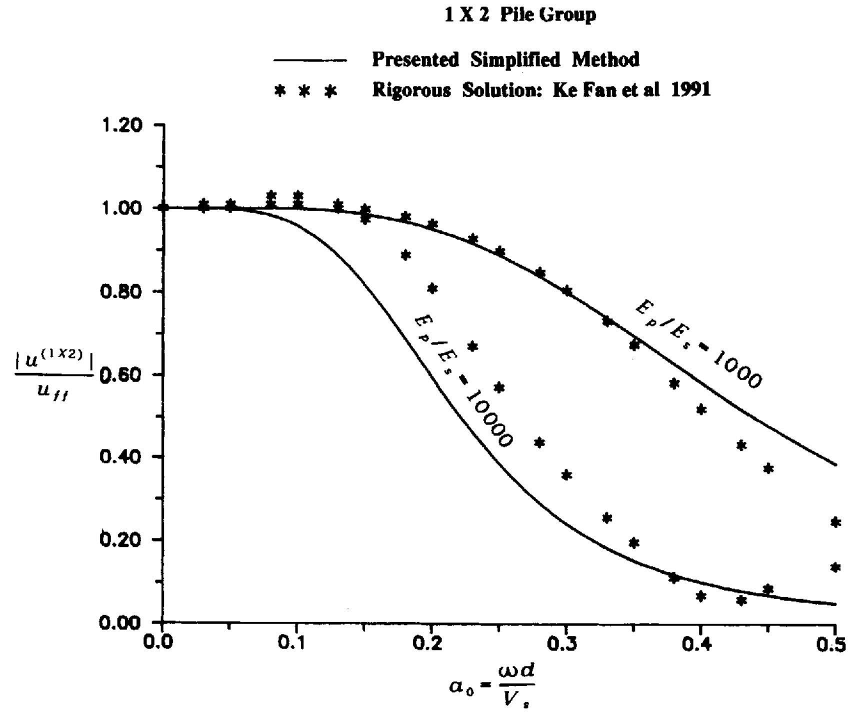

Figure 11. Normalized kinematic seismic response of 1 × 2 fixed-head pile group: comparison of presented method with rigorous results by Ke Fan *et al.* ($\rho_p/\rho_s = 1{\cdot}42$, $L/D = 20$, $\nu = 0{\cdot}4$, $\beta = 0{\cdot}05$)

The solution to equation (37) gives the group displacement U_G and the forces developing at each pile head. Figure 10 plots versus a_0 the ratio of group to free-field displacements for such a 1×3 pile group. The results are compared with the rigorous results of Reference 34; the agreement is very encouraging in view of the simplicity of the developed methods.

The success of the presented approximate method is further illustrated in Figures 11 and 12. Figure 11 plots the same ratio as Figure 10 but for a 1×2 fixed-head pile group, for two values of E_p/E_s, 1000 and 10 000. Figure 12 plots again the same ratio, but for a 2×2 fixed-head pile group for $E_p/E_s = 10\,000$, for two separation distances ($S/d = 5$ and 10). The approximate method captures not only the general trend but also details of the response. For stiffer piles or softer soils the group displacement reduces rapidly as frequency increases. For instance for $E_p/E_s = 10\,000$ the group response is approximately half the free-field response at a frequency of $a_0 = 0{\cdot}25$, whereas for $E_p/E_s = 1000$ the group response is approximately 0·9 times the free-field response at the same frequency ($a_0 = 0{\cdot}25$).

Finally, comparing the group responses (Figures 10, 11, 12) with the single-pile response (Figure 9) one should note that the pile-to-pile interaction effects are rather insignificant for seismic excitation, contrary to head-loading excitation where the pile-to-pile interaction effects are indeed very important. This conclusion,

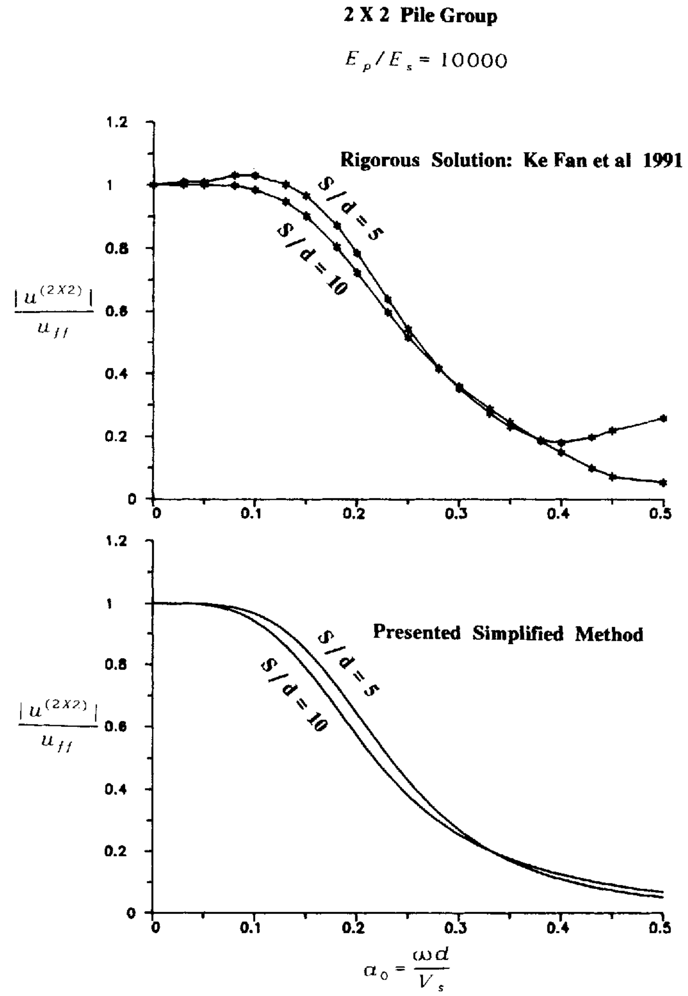

Figure 12. Normalized kinematic seismic response of 2×2 fixed-head pile group: comparison of presented method with rigorous results by Ke Fan *et al.* for two separation distances ($S/d = 5$ and 10) ($\rho_p/\rho_s = 1{\cdot}42$, $L/d = 15$, $\nu = 0{\cdot}4$, $\beta = 0{\cdot}05$)

however, may be applicable only to homogeneous profiles; in heterogeneous deposits, containing consecutive soil layers with drastically different '*acoustic impedances*' (ρV), soil and individual pile seismic displacements are expected to differ sharply at relatively high frequencies and hence to trigger substantial pile-to-pile interaction. Evidence of this for a single pile is presented by Gazetas *et al.*[36]

CONCLUSIONS

A general methodology has been developed to compute dynamic pile–soil–pile interaction problems under both lateral head and seismic loading. The method involves three independent is steps. Pile–soil interaction represented realistically through a dynamic Winkler model and physically-motivated approximations are used to model diffraction and attenuation of waves. Dynamic interaction factors are given by simple closed-form expressions and the group response can be computed simply even by hand calculations. The results obtained are in accord with rigorous solutions, especially for piles in soft and medium-stiff soil $E_p/E_s \geqslant 1000$). It is shown that pile-to-pile interaction effects are significant mainly in the inertial loading creating a strong dependence on frequency of the group efficiency. In seismic loading the ineraction effects between piles in homogeneous structures are very small and could be neglected.

ACKNOWLEDGEMENT

This work was supported by a grant from the Secretariat for Research & Technology of the Greek government.

REFERENCES

1. J. P. Wolf and G. A. Von Arx, 'Impedance function of group of vertical piles', *Proc. ASCE specialty conf. soil dyn. earthquake eng.* **2**, 1024–1041 (1978).
2. A. M. Kaynia and E. Kausel, 'Dynamic stiffness and seismic response of pile groups', *Research Report R82-03*, Massachusetts Institute of Technology Cambridge, Mass., 1982.
3. T. Nogami, H. W. Jones and R. L. Mosher, 'Seismic response analysis of pile-supported structure: assessment of commonly used approximations', *Proc. 2nd int. conf. recent adv. geotech. earthquake eng. soil dyn.* St. Louis 931–940 (1991).
4. M. Novak and M. James, 'Dynamic and static response of pile groups', *Proc. 12th int. conf. soil mech. found. eng.* Rio de Janerio 1175–1178 (1989).
5. G. Waas and H. G. Hartmann, 'Seismic analysis of pile foundations including soil–pile–soil interaction', *Proc. 8th world conf. earthquake eng.* San Francisco **5**, 55–62 (1984).
6. J. M. Roesset, 'Dynamic stiffness of pile groups', *Pile Foundations*, ASCE, New York, 1984.
7. P. K. Banerjee and R. Sen, 'Dynamic behavior of axially and laterally loaded piles and pile groups', *Dynamic Behaviour of Foundations and Buried Structures*, Elsevier Applied Science, New York, 1987, pp. 95–133.
8. R. Dobry and G. Gazetas, 'Simple method for dynamic stiffness a damping of floating pile groups', *Géotechnique* **38**, 557–574 (1988).
9. G. Gazetas and N. Makris, 'Dynamic pile–soil–pile interaction. Part I: Analysis of axial vibration', *Earthquake eng. struct. dyn.* **20**, 115–132 (1991).
10. M. Novak, 'Piles under dynamic loads', *2nd int. conf. recent adv. geotech. earthquake eng. soil dyn.* St. Louis 250–273 (1991).
11. G. W. Blaney, E. Kausel and J. M. Roesset, 'Dynamic stiffness of piles'; *Proc. 2nd int. conf. numer. methods geomech.* Virginia Polytechnic Institute and State University, Blacksburg, VA, II 1010–1012 (1976).
12. R. L. Kuhlemeyer, 'Static and dynamic laterally loaded floating piles', *J. geotech. eng. div. ASCE* **105**, 289–304 (1979).
13. R. Krishnan, G. Gazetas and A. Velez, 'Static and dynamic lateral deflexion of piles in non-homogeneous soil stratum', *Geotechnique* **33**, 307–325 (1983).
14. G. Gazetas and R. Dobry, 'Horizontal response of piles in layered soils', *J. geotech. eng. ASCE* **110**, 20–40 (1984).
15. M. Novak, T. Nogami and F. Aboul-Ella, 'Dynamic soil reactions for plane strain case', *J. eng. mech. div. ASCE* **104**, 953–959 (1978).
16. H. Matlock, H. C. Foo and L. M. Bryant, 'Simulation of lateral pile behavior under earthquake moton', *Proc. ASCE specialty conf. earthquake eng. soil dyn.* **2**, 600–619 (1978).
17. G. A. Blaney and M. W. O'Neill, 'Measured lateral response of mass on single pile in clay', *J. geotech. eng. ASCE* **112**, 443–457 (1986).
18. M. Ochoa and M. W. O'Neill, 'Lateral pile interaction factors in submerged sand', *J. geotech. eng. ASCE* **115**, 359–378 (1989).
19. T. Tazoh, K. Shimizu and T. Wakahara, 'Seismic observations and analysis of grouped piles', *Dynamic Response of Pile Foundations–Experiment, Analysis and Observation, Geotechnical Special Publication No.* 11, ASCE, New York, 1987.
20. J. H. Prevost and R. H. Scanlan, 'Dynamic soil–structure interaction; centrifuge modeling', *Soil dyn. earthquake eng.* **2**, 212–221 (1983).
21. R. F. Scott, J. M. Ting and J. Lee, 'Comparison of centrifuge and full scale dynamic pile tests', *Proc. conf. soil dyn. earthquake eng.* Southampton, U.K. **1**, 299–309 (1982).

22. M. F. Randolf, 'The response of flexible piles to lateral loading', *Géotechnique* **31**, 247–259 (1981).
23. J. M. Roesset and D. Angelides, 'Dynamic stiffness of piles', *Numerical Methods in Offshore Piling*, Institution of Civil Engineers, London, England 1989, pp. 75–80.
24. R. F. Scott, *Foundation Analysis*, Prentice-Hall, Englewood Cliffs, N.J., 1981.
25. J. P. Wolf, *Dynamic Soil–Structure Interaction*, Prentice-Hall, Englewood Cliffs, N.J., 1985.
26. E. Berger, S. A. Mahin and R. Pyke, 'Simplified method for evaluating soil–pile structure interaction effects', *Proc. 9th offshore technol. conf.* 589–598 (1977).
27. J. M. Roesset, 'Stiffness and damping coefficients of foundations', *Special Technical Publication on Dynamic Response of Pile Foundations: Analytical Aspects* (Eds. M. W. O'Neil and R. Dobry) ASCE, New York, 1980.
28. I. Sanchez-Salinero, 'Dynamic stiffness of pile groups: Approximate solutions', *Geotechnical Engineering Report GR83-5*, University of Texas at Austin, 1983.
29. H. G. Poulos and E. H. Davis, *Pile Foundations Analysis and Design*, Wiley, New York, 1980.
30. H. Tajimi, 'Seismic effects on piles', State-of-the-art Report 2, *Proc. specialty session* ICSMFE, 15–26 (1977).
31. T. Kagawa and L. M. Kraft, 'Lateral pile response during earthquakes', *J. geotech. eng. div. ASCE* **107**, 1713–1731 (1981).
32. R. Flores-Berrones and R. V. Whitman, 'Seismic response of end-bearing piles', *J. geotech. eng. div. ASCE* **108**, 554–569 (1982).
33. G. Gazetas, 'Seismic response of end-bearing single piles', *Soil dyn. earthquake eng.* **3**, 82–93 (1984).
34. K. Fan, G. Gazetas, A. Kaynia, E. Kausel and S. Ahmad, 'Kinematic seismic response of single piles and piles groups', *J. geotech. eng. ASCE* **117**, No. 12 (1991).
35. J. M. Roesset, 'Soil amplification of earthquakes', *Numerical Methods in Geotechnical Engineering* (Eds. C. S. Desai and J. T. Christian) McGraw-Hill, New York, 1977.
36. G. Gazetas, K. Fan, T. Tazoh, K. Simizu, & M. Kavvadas, 'Seismic response of soil—pile-foundation—structure systems: some recent developments', ASCE publication on *Piles under Dynamic Loads*, Sept. 1992 (in press).